Supplementary material 1

^{17}O NMR evidence of Free Ionic clusters $Ca^{2+}...CO_3^{2-}$ in silicate glasses: Precursors for carbonate-silicate liquid immiscibility

Yann Morizet[1], Pierre Florian[2], Michael Paris[3], Fabrice Gaillard[4]

(1) Université de Nantes, Nantes Atlantique Universités, Laboratoire de Planétologie et Géodynamique de Nantes (LPG), UMR CNRS 6112, 2 rue de la Houssinière, 44322 NANTES (France)

(2) CNRS-CEMHTI Conditions Extrêmes et Matériaux: Haute Température et Irradiation, UPR 3079, 1D avenue de la Recherche Scientifique, 45071, Orléans, France

(3) Institut des Matériaux Jean Rouxel (IMN), Université de Nantes, UMR CNRS 6502, 2 rue de la Houssinière, BP32229, 44322 NANTES Cedex 3 (France)

(4) CNRS/INSU-Université d'Orléans – BRGM, UMR 7327, Institut des Sciences de la Terre d'Orléans, 1A rue de la Férollerie, 45071, Orléans, France

EXPERIMENTAL AND ANALYTICAL METHODS

High pressure experimental syntheses

The investigated glass compositions were prepared from a mixture of oxides (SiO_2, Al_2O_3 and MgO) and carbonate (Na_2CO_3 and $CaCO_3$) as a source of CO_2. The starting materials were prepared with subsequent enrichment in ^{13}C ($Na_2{}^{13}CO_3$ and $Ca^{13}CO_3$), ^{17}O ($Si^{17}O_2$ and $Al_2{}^{17}O_3$) and ^{29}Si ($^{29}SiO_2$) nuclei. The calculated enrichment is ~40 mol.% and ~15 mol.% relative to total Si and O atoms for ^{29}Si and ^{17}O, respectively. The bulk starting powders contained CO_2 with an excess fluid phase: 18 wt.% CO_2 for HK and XE-2 samples;

40 wt.% for RB8E except RB8E-13 which was prepared with 8.8 wt.% CO_2 to reproduce CO_2 undersaturated conditions.

The experiments were conducted in piston-cylinder apparatus using ¾ inch talc-Pyrex high pressure assemblies between 0.5 and 1.5 GPa for the pressure range and at 1525°C for temperature. Temperatures were monitored by a type B ($PtRh_6$-$PtRh_{30}$) thermocouple accurate to ±5°C. Run durations were at least 30 min to ensure equilibrium (Mysen et al., 1975) then followed by an isobaric quench. An excess fluid phase was witnessed by a large vesicle at the top of each experimental charge.

EPMA and Raman spectroscopy

We used Electron Probe Micro-Analyses (EPMA) to measure the major element concentrations in glasses (see Table 1). Measurements were done on a Cameca SXFive, at 15 kV and 10 nA, with 10 s peak counting time for all elements. Na was analyzed first in defocused mode (20 µm beam diameter) so as to reduce Na elemental loss. The average major elements concentrations for the synthesized glasses were obtained from more than 15 analyses. The error on the chemical composition is on the order of 2% in relative to the value.

The LabRam 300 spectrometer is equipped with a 2400 grooves/mm grating and the spectral resolution is on the order of 1 cm^{-1}. The analyses were performed with a x50 Olympus objective in confocal mode (spatial resolution ~2 µm, depth resolution ~2-5 µm). The Raman signal was collected in between 200 and 1250 cm^{-1}. The output power was set at 125 mW without damaging the glass chips. Several spectra were collected on each glass samples. For each sample, we performed 5-10 scans with an acquisition time of 15 to 60 s.

NMR spectroscopy

All Solid State ^{17}O NMR were conducted on a Bruker 850 MHz Avance III Wide Bore spectrometer operating at a frequency of 115.3 MHz. The ^{17}O spectra were referenced against liquid H_2O at 0 ppm. Full Hahn-echo experiments were conducted using an rf-field of 15 kHz, selective T_{90} pulses of 6.25 µs, an inter-pulse delay of 15 rotor periods (670 µs) and a Double-Frequency Sweeps (DFS) procedure in order to obtain better signal-to-noise for quadrupolar nuclei (Kentgens and Verhagen 1999; Iuga et al. 2000). 1024 transients were accumulated with a recycle delay of 2 s.

{^{27}Al, ^{13}C, ^{29}Si} J-HMQC (Heteronuclear Multiple-Quantum Correlation) experiments (Amoureux et al. 2007; Keeler 2010) were performed using radio-frequency fields of 15 kHz for ^{17}O, 10 kHz for ^{27}Al and 50 kHz for ^{13}C and ^{29}Si. The typical pulse J-HMQC pulse sequence is shown in Figure S1. The J-HMQC experiment uses the so-called scalar coupling ("J") which arises from the electrons involved in the bond between two nuclei and allows the creation of Heteronuclear Multiple-Quantum Coherences. In a {X}-^{17}O J-HMQC experiment where oxygen is the observed nuclei and X the indirect one, the resulting ^{17}O spectrum displays only the oxygen environments that are chemically bounded to X. Excitation times giving the maximum signal were used, corresponding to 220 rotor periods (10 ms) for $^{17}O\{^{27}Al\}$, 551 rotor periods (25 ms) for $^{17}O\{^{13}C\}$ and 771 rotor periods (35 ms) for $^{17}O\{^{29}Si\}$ experiments respectively. A recycle delay of 1 to 3 s is sufficient to retrieve a good S/N and was used throughout the experiment while collecting 32000 transients for $^{17}O\{^{27}Al\}$, 4096 transients for $^{17}O\{^{13}C\}$ and between 10000 to 2000 transients for $^{17}O\{^{29}Si\}$ experiments respectively. DFS was used on the ^{17}O observed channel for all experiments.

CO_2 content determination

We used the method described by Morizet et al. (2013) to determine the CO_2 content via Raman spectroscopy. This Raman calibration for CO_2 content is a linear calibration function such as wt.% CO_2 = 15.17 x CO_3/HF relating the CO_2 content to the ratio between the area of the CO_3^{2-} peak and the high frequency envelop of the silicate glass vibrational signature (CO_3/HF). The calibration was established from a database on CO_2-bearing silicate glasses (65 data points) with CO_2 up to ~16 wt.% CO_2. We extended this Raman calibration to additional CO_2 content data (89 data points) with higher CO_2 content (up to 23 wt.% CO_2) determined using bulk analyzer. The calibration function has been modified according to this new database and the linear relationship is wt.% CO_2 = 13.5 x CO_3/HF; where HF stands for the high-frequency of the symmetric stretch of the aluminosilicate network. Using this method, the typical error on the CO_2 content is 10% in relative to the value. We made an analysis of the typical error with the updated database. The standard deviation on the CO_3/HF ratio is 0.125 and the r^2 parameter is 0.969. As a result, for a CO_3/HF = 1.25, the error is 10% in relative to the value; it will be lower than 10% at higher CO_3/HF and higher than 10% at lower CO_3/HF. In order to be on the safe side, we consider a 10% error in relative to the value for the whole range of CO_3/HF ratio determination. The detail of the update on this calibration can be found in the supplementary material provided in Morizet et al. (2017).

The typical deconvolution of the Raman spectra for the CO_2-bearing glasses is shown in Figure S2. We report the deconvolution all the investigated samples with CO_2 ranging from 2.9 (HK-2) to 13.2 wt.% (HK-M). On each spectrum, we added the derived CO_3/HF ratio from the area of the peaks as well as the calculated CO_2 content using the calibration factor of 13.5 mentioned earlier. The simulation parameters from the deconvolution are provided in Table S1. We can observe that the residual is extremely low therefore attesting of the relevant deconvolution of the Raman spectra and hence a reliable estimate of the glass CO_2 content.

H_2O content determination

The H_2O content in the silicate glasses was determined using Micro-FTIR spectroscopy. The samples were prepared in doubly-polished glass chips for which the thickness of the chips was determined using a Mitutoyo© digitometer with an accuracy of ±1 µm. Analyses were conducted on a ThermoFisher FTIR5700 equipped with a Continuµm microscope. We used a CaF_2 beamsplitter, a MCT-B detector and IR light to cover the 4000-6000 cm^{-1} spectral range. The concentration of OH- (4500 cm^{-1}) and H_2O^{mol} (5200 cm^{-1}) was determined with the Beer-Lambert law (Ohlhorst et al. 2001). The glass density was calculated from the chemical composition with the model of Lange and Carmichael (1990) which includes the change in oxides partial molar volume as a function of pressure and temperature. The model of Lange and Carmichael applies to melt at high temperature however recent work (Guillot and Sator 2007) showed that the change in density in between liquid and glass is small (~10% in relative) towards an increase in density from the liquid to the glass. Therefore, the derived H_2O content with Beer-Lambert law will represent a maximum. We used the linear extinction coefficient applied to Alban Hill phonotephritic glass provided by Behrens et al. (2009): σ_{OH} = 0.62 $L.mol^{-1}.cm^{-1}$ and σ_{H2Omol} = 1.02 $L.mol^{-1}.cm^{-1}$. Those extinction coefficients represent the closest application to the investigated composition. Up to now, there is no extinction coefficient for water species applicable to very low silica melt. The range of water content 0.7 to 1.5 wt.% with a typical error better than 0.2 wt.%. As the experiment were supposed to be conducted under dry conditions, the presence of water is probably due to adsorption of atmospheric H_2O onto the starting material prior capsule preparation and sealing. For such a low silica melt compositions it is almost impossible to produce totally dry silicate glasses. For instance, Moussallam et al. (2015) tried to synthesise

H_2O-free CO_2-rich haplokimberlitic (SiO_2 < 40 wt.%) glass and the recovered glasses contained between 0.5 and 1.7 wt.% H_2O even using cautious capsule preparing method.

Complementary {X}-^{17}O J-HMQC NMR data

In this supplementary material, we provide complementary NMR data which includes the Echo MAS and {X}-^{17}O J-HMQC NMR spectra not shown in the main text of the manuscript. Those spectra are reported in Figure S3 for HK-2, RB8E-7 and RB8E-13. The spectra obtained for these three samples are similar to the ones reported in the main manuscript, hence corroborating the fact that CO_2 dissolves in low silica melt as FIC $M^{n+}..CO_3^{2-}$.

In a similar way, we provide in Figure S4 the relevant deconvolution of the ^{17}O MAS NMR spectra not reported in the main manuscript: RB8E-7, RB8E-13, HK-2 and HK-M. As stated in the manuscript, the ^{17}O MAS NMR spectra of Mg-bearing (HK) are only partially reproduced; as can be seen from Figure S4 there is a residual signal located at ~+70 ppm which we could be assigned to MgO_x polyhedra (Kohara et al. 2004, 2011; Benmore et al. 2011; Wilding et al. 2012); however, further is required to definitely propose an assignment. The ^{17}O MAS NMR spectrum of Mg-free RB8E-13 is not reproduced adequately. For instance, as seen in Figure S4, there is an important residual broad and centered at ~+20 ppm which appears not to be reproduced by the combination of Gaussian lines derived from the {X}-^{17}O J-HMQC spectra deconvolution. Such signal at ~+20 ppm could be attributed to oxygen triclusters (O^{III}) which have been identified in silicate glasses (Stebbins et al. 2001; Benoit et al. 2005; Iuga et al. 2005).

We have acquired 2D {^{27}Al}-^{17}O J-HMQC NMR spectra for several investigated glasses in order to determine the origin of the asymmetry observed in the 1D {^{27}Al}-^{17}O J-

HMQC NMR (see Figure 1). The 2D spectra for HK-1 and RB8E-12 are shown in Figure S5. We observe in Figure S5 that there are three individual signals in the $\{^{27}Al\}$-^{17}O J-HMQC NMR spectra. The peak maximum in the ^{27}Al dimension of those signals is located at +61.2, +29.9 and +1.7 ppm. Those peaks are assigned the ^{17}O atoms linked to Al atoms in different coordination from 4-coordinated to 6-coordinated Al (Stebbins et al. 2000). The peaks are observed in both Mg-bearing (HK-1) and Mg-free (RB8E-12) compositions; however, the 5- and 6-coordinated Al appears more intense in Mg-bearing HK-1 as compared to the Mg-free RB8E-12 glass. The observed higher degree of Al coordination in Mg-rich composition is in agreement with previous work (Kjeldsen et al. 2013). As the contribution of each Al signal is summed to the ^{17}O dimension, it results a slight asymmetry of the ^{17}O signal as inferred in Figure 1.

REFERENCES CITED

Behrens, H., Misiti, V., Freda, C., Vetere, F., Botcharnikov, R.E. , Scarlato, P., 2009 Solubility of H_2O and CO_2 in ultrapotassic melts at 1200 and 1250 °C and pressure from 50 to 500 MPa. Am. Mineral. 94, 105–120.

Benmore, C.J., Soignard, E., Guthrie, M., Amin, S.A., Weber, J.K.R., McKiernan, K., Wilding, M.C., and Yarger, J.L. (2011) High pressure x-ray diffraction measurements on Mg_2SiO_4 glass. Journal of Non-Crystalline Solids 357, 2632-2636.

Benoit, M., Profeta, M., Mauri, F., Pickard, C.J., and Tuckerman, M.E. (2005) First-principles calculation of the ^{17}O NMR parameters of a calcium aluminosilicate glass. Journal of Physical Chemistry B 109, 6052–6060.

Guillot, B., and Sator, N. (2007) A computer simulation study of natural silicate melts. Part II: high pressure properties. Geochimica et Cosmochimica Acta 71, 4538–4556.

Iuga, D., Schäfer, H., Verhagen, R., and Kentgens, A.P. (2000) Population and coherence transfer induced by double frequency sweeps in half-integer quadrupolar spin systems. Journal of Magnetic Resonance 147, 192-209.

Iuga, D., Morais, C., Gan, Z., Neuville, D.R., Cormier, L., and Massiot, D. (2005) NMR Heteronuclear Correlation between quadrupolar nuclei in solids. Journal of American Chemical Society 127, 11540–11541.

Kentgens, A.P.M., and Verhagen, R. (1999) Advantages of double frequency sweeps in static, MAS and MQMAS NMR of spin I=3/2 nuclei. Chemical Physics Letters 300, 435-443.

Kjeldsen, J., Smedskjaer, M.M., Mauro, J.C., Youngman, R.E., Huang, L., and Yue, Y. (2013) Mixed alkaline earth effect in sodium aluminosilicate glasses. Journal of Non-Crystalline Solids 369, 61-68.

Kohara, S., Suzuya, K., Takeuchi, K., Loong, C.-K., Grimsditch, M., Weber, J.K.R., Tangeman, J.A., and Key, T.S. (2004) Glass formation at the limit of insufficient network formers. Science 303, 1649-1652.

Lange, R., and Carmichael, I.S.E. (1990) Thermodynamic properties of silicate liquids with emphasis on density, thermal expansion and compressibility. In J. Nicholls and J.K. Russell, Eds., Modern Methods of Igneous Petrology: Understanding Magmatic Processes, 24, p. 25–64. Reviews in Mineralogy, Mineralogical Society of America, Chantilly, Virginia.

Morizet, Y., Brooker, R.A., Iacono-Marziano, G., and Kjarsgaard, B. (2013) Quantification of CO_2 dissolved in silicate glasses of various compositions with Micro-Raman spectroscopy. American Mineralogist 98, 1788–1802.

Morizet, Y., Paris, M., Sifré, D., Di Carlo, I., and Gaillard, F. (2017) The effect of Mg concentration in silicate glasses on CO_2 solubility and solution mechanism: Implication for natural magmatic systems. Geochimica et Cosmochimica Acta 198, 115-130.

Mysen, B.O., Arculus, R.J., and Eggler, D.H. (1975) Solubility of carbon dioxide in natural nephelinite, tholeiite and andesite melts to 30 kbar pressure. Contributions to Mineralogy and Petrology 53, 227–239.

Ohlhorst, S., Behrens, H., and Holtz, F. (2001) Compositional dependence of molar absorptivities of near-infrared OH− and H_2O bands in rhyolitic to basaltic glasses. Chemical Geology 174, 5–20.

Schurko, R.W., Hung, I., and Widdifield, C.M. (2003) Signal enhancement in NMR spectra of half-integer quadrupolar nuclei via DFS-QCPMG and RAPT-QCPMG pulse sequences. Chemical Physics Letters 379, 1-10.

Stebbins, J.F., Kroeker, S., Lee, S.K., and Kiczenski, T.J. (2000) Quantification of five- and six-coordinated aluminum in aluminosilicate and fluoride-containing glasses by high-field, high-resolution ^{27}Al NMR. Journal of Non-Crystalline Solids 275, 1–6.

Stebbins, J.F., Oglesby, J.V., and Kroeker, S. (2001) Oxygen triclusters in crystalline $CaAl_4O_7$ (grossite) and calcium aluminosilicate glasses: oxygen-17 NMR. American Mineralogist 86, 1307–1311.

Wilding, M., Guthrie, M., Kohara, S., Bull, C.L., Akola, J., and Tucker, M.G. (2012) The structure of MgO-SiO_2 glasses at elevated pressure. Journal of Physics Condensed Matter 24, 225403-225444.

Table S1: Derived parameters from the Raman spectra deconvolutions.

Raman parameters*	HK-1	HK-2	HK-M	RB8E-7	RB8E-12	RB8E-13	XE-2
				Peak 1 ν_1 CO_3^{2-}			
Pos.	1080.9	1079.1	1082.7	1069.4	1074.9	1068.4	1080.7
FWHM	39.1	37.0	38.1	35.7	31.6	34.0	41.4
				Peak 2 Q^n			
Pos.	1056.1	1052.3	1046.9	1033.3	1041.4	1038.5	1060.9
FWHM	66.8	65.2	72.6	64.8	59.5	57.0	59.5
				Peak 3 Q^n			
Pos.	989.9	980.0	972.6	974.0	967.6	962.8	993.1
FWHM	62.9	61.4	55.0	58.6	59.2	59.6	62.8
				Peak 4 Q^n			
Pos.	940.7	926.9	920.3	925.4	918.7	913.0	937.0
FWHM	63.4	61.1	58.6459	58.9	52.0	53.4	62.8
				Peak 5 Q^n			
Pos.	874.0	866.9	863.6	865.4	865.3	860.6	878.9
FWHM	62.7	57.6	55.4	58.6	54.0	54.9	61.6
CO_3/HF†	0.525±0.006	0.213±0.018	0.970±0.014	0.481±0.013	0.936±0.043	0.565±0.104	0.312±0.006
Wt.% CO_2‡	7.1±0.1	2.9±0.2	13.2±0.2	6.5±0.2	12.6±0.6	7.7±1.4	4.2±0.1

* The reported Raman parameters (pos. and FWHM) were obtained from the deconvolution of the Raman spectra. The error associated to the values does not exceed ±0.5 cm^{-1} as provided by the software package (Origin© 7.5).

† The CO_3/HF values are calculated from the derived areas. The reported error corresponds to the standard deviation of the ratio calculated from replicated spectra.

‡ The CO_2 content is determined with the following relation wt.% CO_2 = 13.5 x CO_3/HF.

Supplementary Figures:

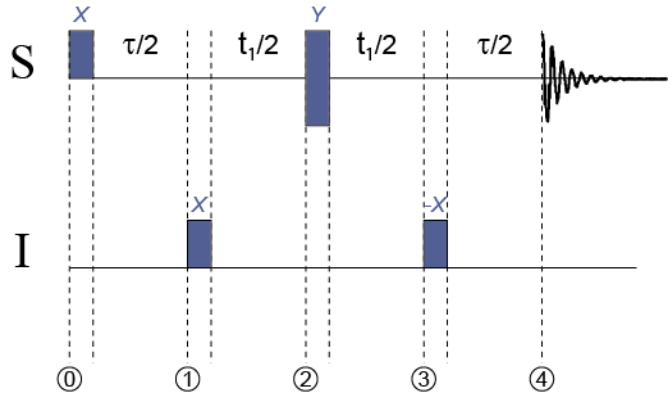

Figure S1: Typical J-HMQC NMR pulse sequence. The excitation is transferred from the I nuclei and acquisition is made subsequently on the S nuclei.

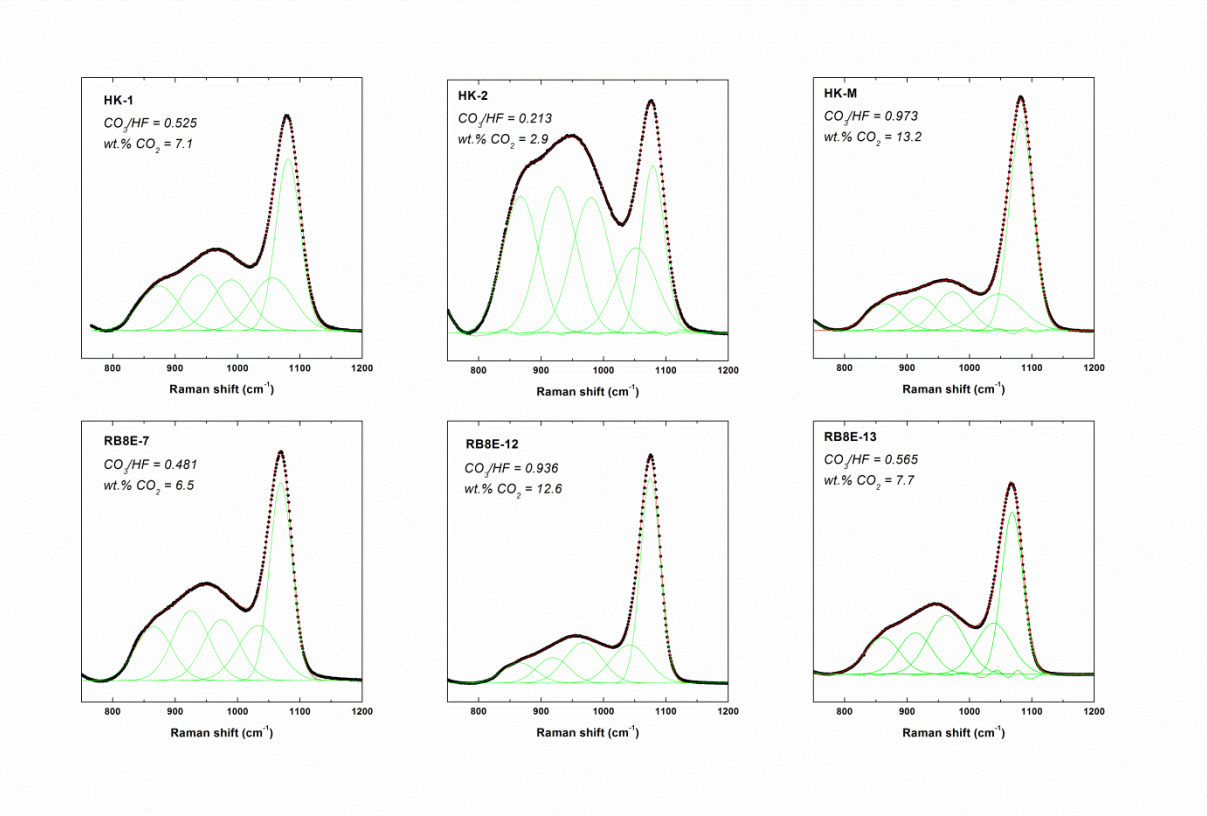

Figure S2: Glass sample Raman spectra simulated with five Gaussian lines corresponding to the symmetric stretch of the CO_3^{2-} group (ν_1 CO_3^{2-}) and silicate network (ν_1 Q^n). The simulation is reported for the investigated samples. The ratio CO_3/HF is reported next to each simulation and is used to calculate the CO_2 content from the linear correlation (see text for detailed discussion).

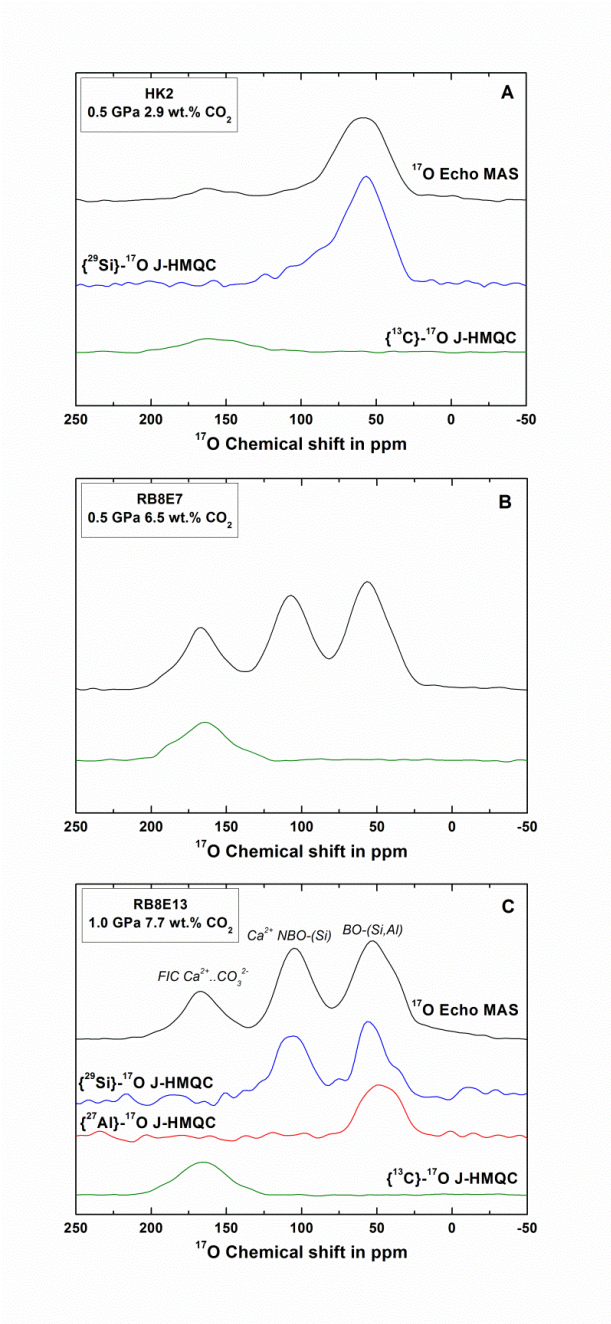

Figure S3: ^{17}O Full Hahn-Echo MAS and $\{^{13}C\}$- $\{^{27}Al\}$- $\{^{29}Si\}$-^{17}O J-HMQC NMR spectra of CO_2-bearing silicate glasses: HK-2 (A), HK-1 (B), RB8E-7 (B) and RB8E-13 (C). Three oxygen environments are identified with Full Hahn-Echo MAS spectra: FIC $M^{n+}..CO_3^{2-}$, Ca^{2+} NBO-Si and BO-(Si,Al).

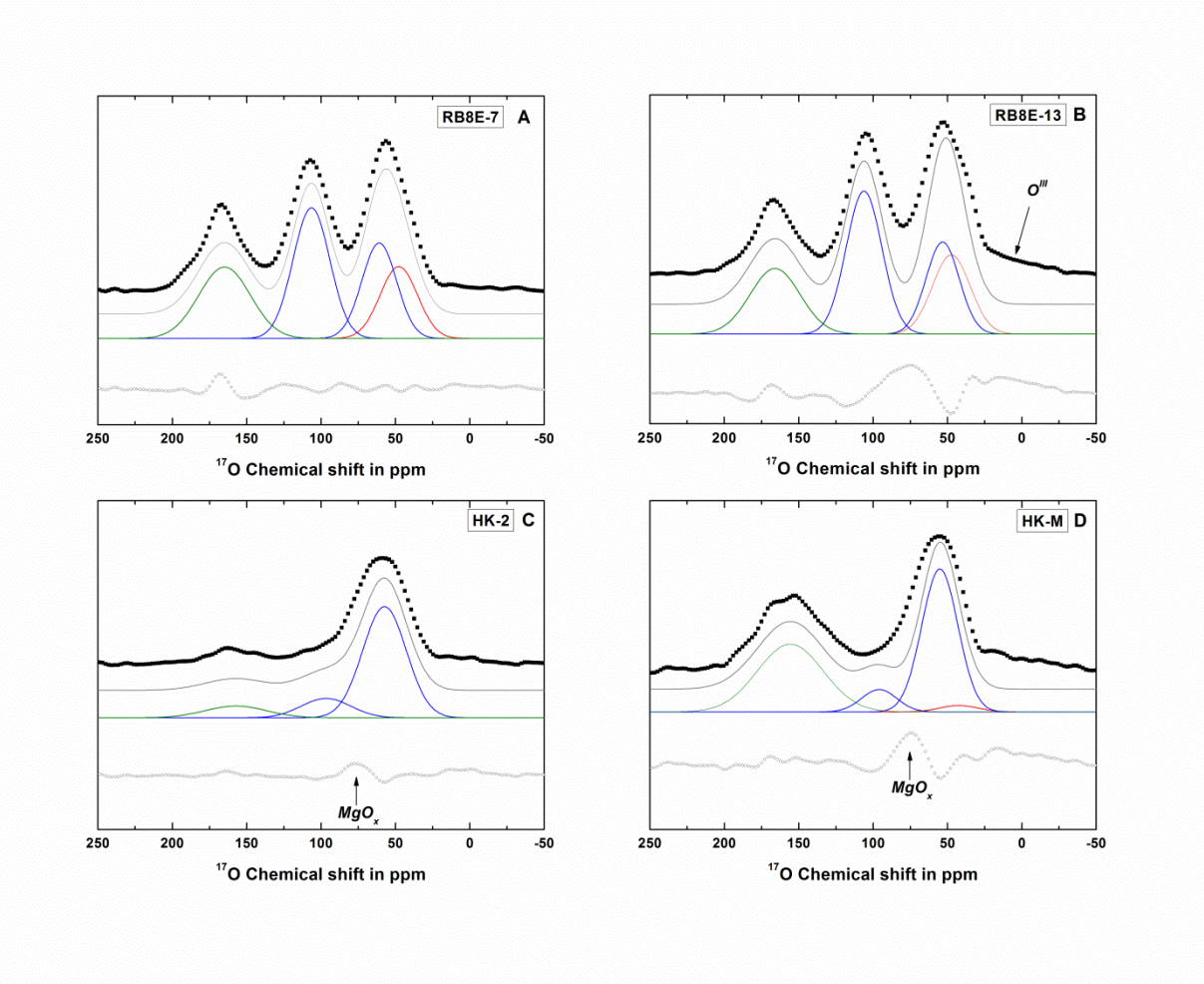

Figure S4: ^{17}O MAS spectrum reconstruction from Gaussian lines derived from {X}-^{17}O J-HMQC spectra. The deconvolution consists in one line for FIC $M^{n+}..CO_3^{2-}$ group; one line for oxygens in NBO configuration linked to Si atoms; two line for oxygens in BO configuration associated to Si and Al atoms. The residuals exhibit a line located at ~+70 ppm which is not accounted for by the proposed deconvolution and which could be attributed to oxygen atoms in MgO_x configuration.

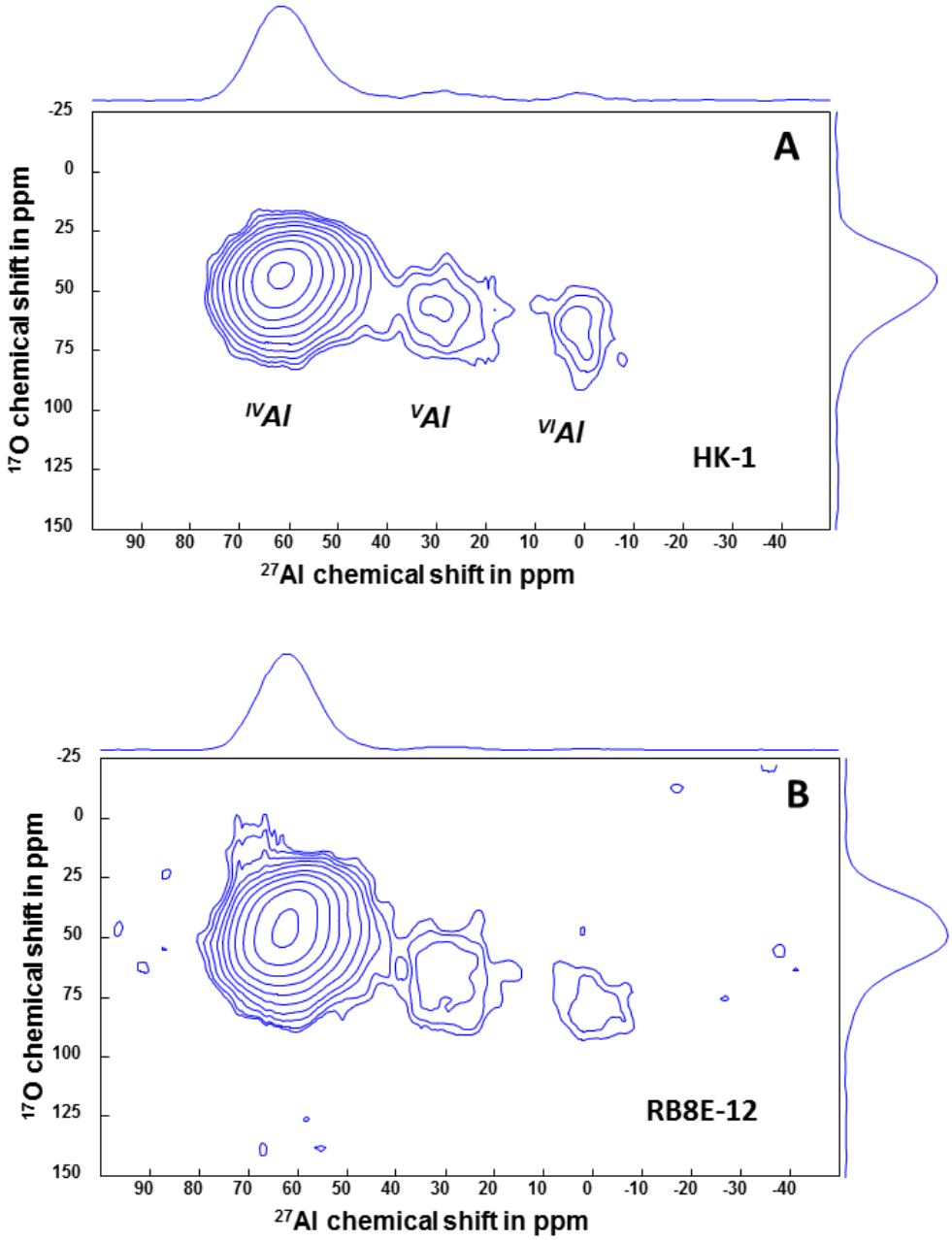

Figure S5: 2D {^{27}Al}-^{17}O J-HMQC NMR spectra for HK-1 ane RB8E-12 samples. Three individual lines can be observed in the ^{27}Al dimension and corresponding to Al atoms in different coordination (4- to 6-coordinated) within the glass structure. Due to strong overlapping, only an asymmetric line is observed in the ^{17}O dimension.